

Theoretical Characterization of Photoisomerization Channels of Dimethylpyridines on the Singlet and Triplet Potential Energy Surfaces

Zexing Cao,^{*[a]} Qianer Zhang,^[a] and Sigrid D. Peyerimhoff^[b]

Abstract: Photoexcitations and photoisomerizations due to low-lying $n\pi^*$ and $\pi\pi^*$ excited states of dimethylpyridines are investigated by density functional theory, CASSCF, CASPT2 and MRCI methodologies. Mechanistic details for the formation of Dewar dimethylpyridines and the interconversions of dimethylpyridines are rationalized through the characterization of minima and transition states on the singlet and triplet potential energy surfaces of relevant intermediates. Our present theoretical schemes suggest that Möbius dimethylpyridine intermediate **14** and azabenzvalene intermediate **10** can serve as possible precursors to Dewar dimethylpyridines and singlet phototransposition

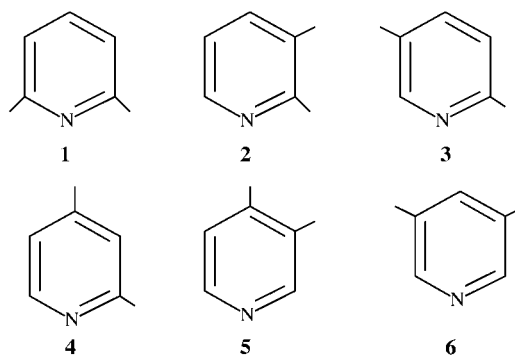
products, respectively. The calculations suggest that an $S_1(\pi\pi^*)/S_0$ conical intersection in dimethylpyridines **2** is involved in the formation of **14**. An azabenzvalene **10** might be formed through $S_2(\pi\pi^*)/S_1(n\pi^*)$ interaction followed by an S_1/S_0 decay in dimethylpyridine **6**. Calculated barriers of isomerizations from **14** to Dewar dimethylpyridine **7** and from **10** to **4** are 8.4 and 28.5 kcal mol⁻¹ at the B3LYP/6-311G** level, respectively. In the suggested

Keywords: ab initio calculations • dimethylpyridine • isomerization • photochemistry • photoisomerization

triplet multistage transposition mechanism, an out-of-plane distorted geometry **19** due to vibrational relaxation of the $T_1(^3B_1)$ excited state of 3,5-dimethylpyridine **6** is a precursor of the interconversion of **6** to 2,4-dimethylpyridine **4**. The formation of a triplet azaprefulvene **21** with a barrier of 20.7 kcal mol⁻¹ is a key step during the triplet migration process leading to another out-of-plane distorted structure **27**. Subsequent re-aromatization of **27** completes the interconversion of **6** with **4**. Present calculations provide some insight into the photochemistry of dimethylpyridines at 254 nm.

Introduction

Pyridine and its methyl derivatives are important heteroaromatic molecules. The photophysics and photochemistry of these nitrogen heterocycles have both received considerable attention experimentally.^[1-6] In recent experiments, Pavlik et al.^[6] studied the photochemistry of dimethylpyridines **1–6** in the vapor phase and in solution by irradiation at 254 nm and discovered new features in the photoisomerization reactions. For example, when 2,3-dimethylpyridine (**2**) is irradiated at 254 nm in CD₃CN at -30 °C, only the Dewar pyridine isomer **7** resulting from 3,6-bonding (Scheme 1) was observed by ¹H NMR spectroscopy. Irradiation of dimethylpyridine **6** vapors at 254 nm results in the formation of methyl transposition products **3** and **4** (Scheme 2) in yields of 14.7% and

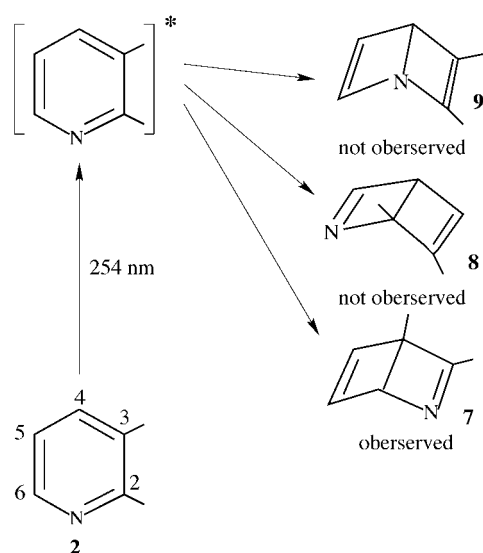
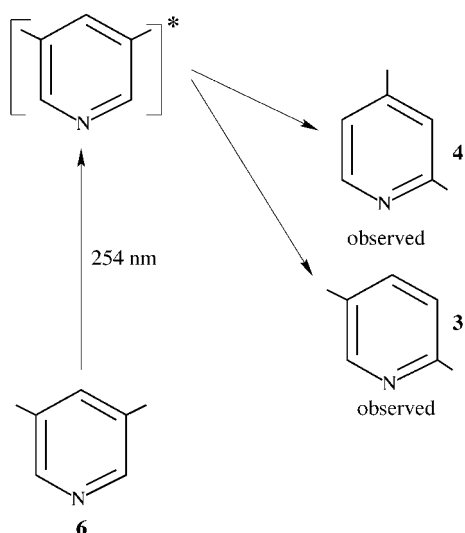


12.7%, respectively. On the other hand, when the reactant **6** is irradiated at wavelengths > 290 nm, no isomerization occurs.

Since the π -electronic structures of dimethylpyridines are similar to those of pyridine, the photoexcitations of the six different dimethylpyridines should be comparable to those of pyridine. Extensive experimental and theoretical investigations into the electronic spectrum of pyridine show that the two lowest singlet $n-\pi^*$ and $\pi-\pi^*$ excitations occur at 4.59 and 4.99 eV,^[7-11] and the lowest triplet-singlet absorptions appear in the region 3.7–4.1 eV,^[8,9] even though the assignment of the lowest triplet state as $\pi\pi^*$ or $n\pi^*$ depends on

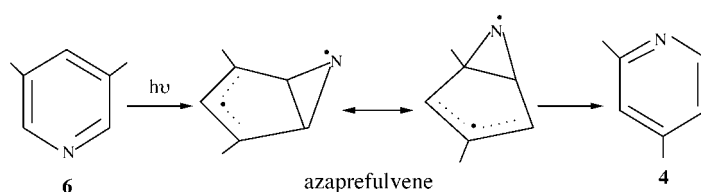
[a] Dr. Z. Cao, Prof. Q. Zhang
Department of Chemistry, State Key Laboratory for Physical Chemistry of the Solid Surface,
Xiamen University, Xiamen 361005 (China)
Fax: (+86)592-2183043
E-mail: zxcao@xmu.edu.cn

[b] Prof. Dr. S. D. Peyerimhoff
Institut für Physikalische und Theoretische Chemie,
Universität Bonn, Wegelerstrasse 12, 53115 Bonn (Germany)
Fax: (+49)228-739-064

Scheme 1. Irradiation of **2** at 254 nm.Scheme 2. Irradiation of **6** at 254 nm.

details of the theoretical approaches.^[10, 11] Methyl substitution in pyridine might change the energy of excited states slightly due to the methyl hyperconjugation, but the basic photoexcitation features are not expected to change significantly. For example, the observed excitations from the ground state to $S_1(n\pi^*)$ and $S_2(\pi\pi^*)$ states in 2,6-dimethylpyridine (**1**) occur at 4.36 and 4.58 eV, respectively,^[12] that is 0.23 eV and 0.41 eV lower than the singlet $n-\pi^*$ and $\pi-\pi^*$ excitations in pyridine.

In consideration of the mechanistic aspects, Pavlik et al.^[6] proposed a scheme for the photochemical reaction of **6** to **4**, involving electrocyclic ring closure, nitrogen migration around the sides of the cyclopentenyl ring, and rearomatization. In this scheme, an azaprefulvene species with biradical character, originating from the excited state $S_2(\pi\pi^*)$, is suggested to be a precursor in the interconversion of the dimethylpyridines (Scheme 3). Similar mechanisms were previously used to explain photoisomerization of five- and six-membered heteroaromatic compounds and isomeric cy-

Scheme 3. Proposed mechanism for the formation of **4** from **6** via an azaprefulvene.

notoluenes.^[13, 14] A recent study of femtosecond dynamics as well as theoretical calculations of pyridine by Zewail and Chachisvilis^[5] explored the photochemical dynamics of the $S_2(\pi\pi^*)$ excited state leading to formation of the azaprefulvene isomer. The reaction path on the $S_2(\pi\pi^*)$ potential energy surface (PES) was found to be the lowest path for the formation of the azaprefulvene isomer at the CASSCF(8,7)/STO-3G level.^[5]

Formation of Dewar pyridine intermediates was assumed to occur^[6] by intersystem crossing with a triplet excited state T_1 . In an earlier study, Caplain and Lablache-Combiere^[1] suggested a ring-transposition mechanism involving azaprismane intermediates in order to rationalize the observed photoisomerizations. However, this azaprismane intermediate-mediated scheme may cause some mechanistic ambiguities.^[6] Since the observed excitation energy to the lowest triplet state ranges from 3.69 eV (336 nm) to 4.1 eV (302 nm)^[8, 9] in pyridine, the critical irradiation light of 290 nm for the photoreaction of **6** corresponds to an energy of 4.27 eV, that is higher than the onset of the triplet state if the same location is assumed as in pyridine. If excitation of dimethylpyridines with light of 254 nm populates the lowest triplet state T_1 , this state is expected to have excess vibrational energy. This excess vibrational energy may be important for photoisomerization reactions.

Previous theoretical calculations^[15] at the UHF/STO-3G level investigated the formation of this azaprefulvene species via the $S_2(\pi\pi^*)$ state of pyridine, crossing both the $S_1(n\pi^*)$ and S_0 states along a concerted pathway. In an MC-SCF study on the photoreaction of benzene,^[16a] a similar biradical prefulvene of benzene was found to be a transition state, whilst this azaprefulvene structure was characterized as a minimum in previous studies.^[15, 16b] The reaction path (IRC) from prefulvene in the benzene reaction leads to a minimum structure, termed prebenzvalene. This metastable prebenzvalene has almost the same energy and geometry as the prefulvene structure. The conversion from this prebenzvalene to a more stable photoproduct benzvalene is quite facile.^[16a] CASSCF and MP2 calculations by Johnson and Daoust^[17] show that the conversion from Dewar benzene to benzene can occur on the singlet PES via a Möbius-benzene intermediate.

To rationalize these photochemical processes, we performed a theoretical investigation of the photoisomerizations of dimethylpyridines outlined in Schemes 1 and 2. Relevant valence-shell electronic spectra were determined by CASPT2 and MRCI calculations. Conical crossing structures leading to the Möbius-dimethylpyridine intermediate and azabenzvalene intermediate were characterized. Plausible reaction pathways and singlet and triplet intermediates involved in the photoisomerization are proposed.

Computational Details

Geometry optimizations and vibrational analyses for stationary points on the potential energy surfaces (PESs) of the singlet and triplet states have been performed based on density functional theory (DFT), specifically the Becke's three-parameter hybrid exchange functional^[18] and the Lee–Yang–Parr correlation functional^[19] (B3LYP). For the triplet states and the singlet biradical structures, the Hartree–Fock exchange potential from the unrestricted wavefunction is employed in the Becke's hybrid exchange functional (UB3LYP). For comparison with the B3LYP calculations, the CASSCF method was also used for geometry optimization of the dimethylpyridine isomers (**1–6**). In this case, the CASSCF active space consists of six π orbitals and a lone pair (sp^2 -like hybrid orbital) of nitrogen, so that eight electrons were allowed to be distributed into seven molecular orbitals, denoted as CAS(8,7). The location of conical crossing structures and the optimization of singlet biradical azaprefulvene and preazabenzvalene structures were determined by CAS(6,6) calculations. This choice seemed sufficient because the lowest and highest molecular orbitals in the active space of the CAS(8,7) calculations were found to have negligible contribution to the CASSCF wavefunction. Excitation energies for relevant singlet and triplet excited states were calculated by CASPT2^[20] and MRCI methods.^[21] In the MRCI calculations, the core and lowest five valence molecular orbitals are always kept doubly occupied so that 32 valence electrons are active. The threshold value for configuration selection was generally 10^{-7} hartree. A Davidson-type procedure was employed to estimate the full CI limit.^[22] All DFT and CASSCF calculations were performed with the Gaussian 94 package^[23] employing the 6–311G** basis set.^[26, 27] MOLCAS 4.0^[24] and DIESEL-CI programs^[25] were used for the CASPT2 and MRCI calculations. In these cases the 9s5p/5s3p^[28] for carbon and nitrogen augmented with one d-polarization function (exponent 0.75) was employed, since this basis set has been found to perform very successfully for electronically excited state. For hydrogen atoms, the STO-6G basis set was considered here. The smaller standard 6–31G basis set was used for the search of selected excited states and conical intersections in the CAS(6,6) calculation.

Results and Discussion

Geometry and stability of dimethylpyridines: The optimized geometries of the dimethylpyridines (**1–6**) as obtained for the DFT/B3LYP calculations are displayed in Figure 1. The CAS(8,7) calculations for dimethylpyridines give almost the same equilibrium parameters. Relative energies at different levels of theory are shown in Table 1. The 2,6-dimethylpyr-

Table 1. Relative energies [kcal mol^{-1}] of dimethylpyridines.

Species	SCF	CASSCF(8,7)	B3LYP ^[a]
1	0.00	0.00	0.00
2	3.38	2.73	2.36(2.77)
3	2.71	1.82	1.91(2.01)
4	1.28	1.20	1.30(1.41)
5	4.22	3.34	3.38(3.92)
6	4.70	3.29	3.61(3.80)

[a] Values in parentheses from zero-point vibrational energy correction.

idine (**1**) is predicted to be the most stable isomer in all treatments. Furthermore, it is seen that the relative energies of the B3LYP calculations are in good agreement with the results of the more demanding CAS(8,7) calculations. All isomers are within an energy range of 4 kcal mol^{-1} from each another. The second most stable isomer **4** lies only 1.4 kcal mol^{-1} above the lowest energy structure, while isomers **5** and **6** are the least preferred arrangements

according to the present calculations. From Table 1 it is seen that a relatively large zero-point energy effect exists in the isomers **2** and **5**. This can be ascribed to a crowded arrangement of two methyl groups in both isomers.

Electronic spectra of valence-shell excitations: Excitation energies and oscillator strengths due to $\pi-\pi^*$ and $n-\pi^*$ transitions in dimethylpyridines **2** and **6** as determined by CASPT2 and MRCI calculations are given in Table 2. At the CASPT2 (MRCI) level, the lower $n-\pi^*$ and $\pi-\pi^*$ excitations

Table 2. Selected vertical excitation energies [eV/nm] and oscillator strengths of dimethylpyridines **2** and **6**.

State		CASPT2	MRCI	$f(\text{CASPT2/MRCI})$
dimethylpyridine 2				
2 ¹ A'	$\pi \rightarrow \pi^*$	5.11/242.6	5.13/242	0.031/0.117
2 ¹ A''	$n \rightarrow \pi^*$	5.19/238.9	5.21/238	0.002/0.006
2 ¹ A''	$n \rightarrow \pi^*$	5.52/224.6	5.71/217	0.00005/0.00002
1 ³ A'	$\pi \rightarrow \pi^*$	4.14/299.5	4.32/287	
1 ³ A''	$n \rightarrow \pi^*$	4.28/289.7	4.35/285	
dimethylpyridine 6				
1 ¹ B ₁	$n \rightarrow \pi^*$	4.45/278.6	4.78/259.4	0.019/0.006
1 ¹ B ₂	$\pi \rightarrow \pi^*$	4.89/253.6	4.83/256.7	0.033/0.047
1 ¹ A ₂	$n \rightarrow \pi^*$		5.99/207.0	/0.0
1 ¹ A ₁	$\pi \rightarrow \pi^*$		6.83/181.5	/0.862
1 ³ B ₁	$n \rightarrow \pi^*$	4.29/289.0	4.39/282.4	
1 ³ A ₁	$\pi \rightarrow \pi^*$	4.33/286.3	4.37/283.7	
1 ³ B ₂	$\pi \rightarrow \pi^*$	4.52/274.3	4.91/252.5	
1 ³ A ₂	$n \rightarrow \pi^*$	5.12/242.2	5.90/210.2	

in **6** occur at 4.45 (4.78) and 4.89 (4.83) eV, respectively. For **2**, the $n-\pi^*$ and $\pi-\pi^*$ bands are predicted to center at 5.19 (5.21) and 5.11 (5.13) eV, respectively. Hence the S₁ excited state in **6** arises from the $n-\pi^*$ excitation, and in **2** from the $\pi-\pi^*$ excitation. On the other hand, the separation between the $\pi\pi^*$ and $n\pi^*$ states in **2** and **6** is only 0.08 (0.08) and 0.44 (0.05) eV at the CASPT2 (MRCI) level, respectively. In a previous theoretical study on pyridine^[11] the CASPT2 calculated transition energies are generally in very good agreement with the experimental data for most excited states, although deviations within ± 0.3 eV occur for some excited states, including $n-\pi^*$ excitations.

The vertical singlet–triplet $n-\pi^*$ transition from the ground state ¹A₁ of **6** to the excited state ³B₁ occurs at 4.29 eV/289 nm (4.39 eV/282 nm) at the CASPT2 (MRCI) level. The singlet–triplet $\pi-\pi^*$ transition lies at 4.33 eV/286 nm (4.37 eV/284 nm). Both $n\pi^*$ and $\pi\pi^*$ triplet excited states are found to be nearly degenerate in energy. A similar feature for the triplet excited states of dimethylpyridine **2** is seen (Table 2). Considering the effect of methyl substitution on excitation energies, both vertical singlet–triplet excitations should be comparable with the experimental bands found between 3.7–4.1 eV for the singlet–triplet excitation of pyridine.^[9, 11] These singlet and triplet states are accessible energetically by the irradiation light of 254 nm (4.88 eV) used in the recent study of vapor-phase photochemistry of dimethylpyridines,^[6] and are thus expected to be involved in the photoisomerization of dimethylpyridines at 254 nm. As expected, the $\pi-\pi^*$ transitions have the largest transition probabilities.

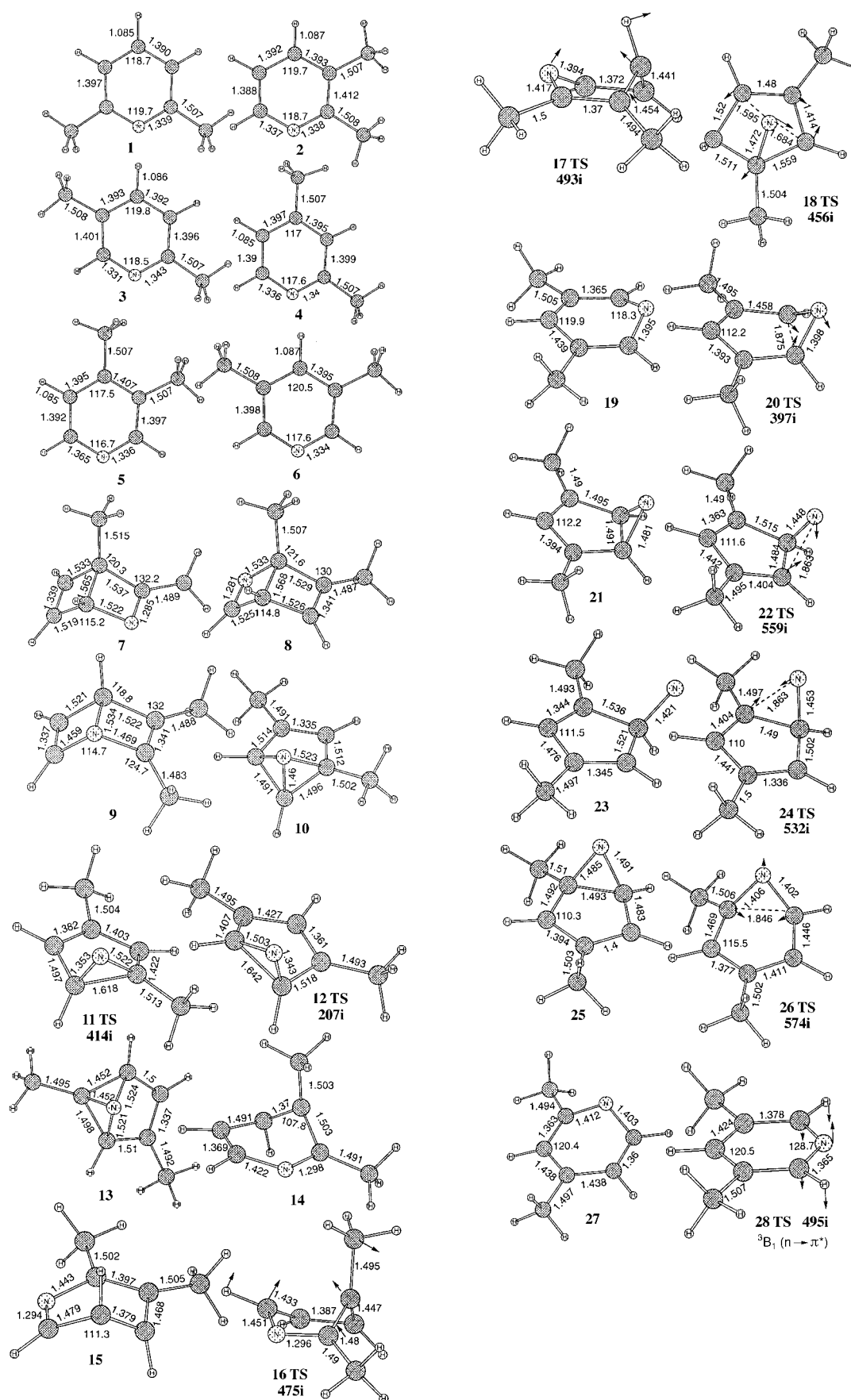


Figure 1. B3LYP/6-311G**-optimized geometries [Å, °] of singlet (1–18) and triplet states (19–28).

Geometrical features of the excited states: To gain some insight into the geometry of the $n\pi^*$ and $\pi\pi^*$ excited states of dimethylpyridines, we optimized the $S_1(\pi\pi^*)$ excited state ${}^1A'$ of **2** and the $S_1(n\pi^*)$ excited state 1B_1 of **6** by CAS(8,7)/6–31G calculations. These lowest $n\pi^*$ and $\pi\pi^*$ excited states play an important role in the suggested schemes for the formation of intermediates **14** and **10** (vide infra). Figure 2 shows the

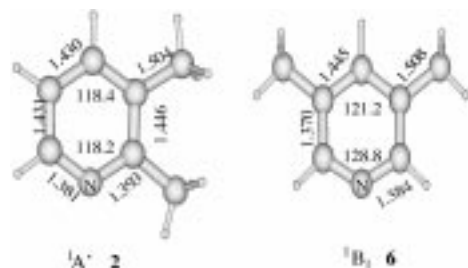


Figure 2. CASSCF-optimized geometries [\AA , $^\circ$] of the excited states.

geometries of both excited states. Compared to the geometries of the ground states of **2** and **6** in Figure 1, the $\pi-\pi^*$ excitation results in stretching dimethylpyridine CC and CN bonds in the excited state ${}^1A'$, while the $n-\pi^*$ excitation leads to the excited state 1B_1 of **6** with shorter 2–3 and 5–6 bonds and longer 1–2, 1–6, and 3–4, 4–5 bonds. This is in agreement with the bonding features of molecular orbitals π and π^* presented in previous study by Sobolewski and Domcke.^[15] The geometric behavior of the $\pi\pi^*$ and $n\pi^*$ states in the other isomers is expected to show the equivalent trends. Vibrational frequency calculations show that both excited states S_1 and S_2 are stable minima on the PESs. The significant change in geometry between the ground and excited states will result in a considerable difference between the adiabatic and vertical transition energies. This relatively low adiabatic transition energy was also seen in the CASPT2 calculation of pyridine.^[11]

Formation of intermediates Möbius dimethylpyridine and dimethylazabenzvalene structures: Möbius benzene and benzvalene were proposed as photoproducts of benzene, and precursors to other benzene valence isomers.^[17, 29–30] A prefulvene structure was proposed to be involved in the formation of benzvalene.^[16a] Previous calculations by Sobolewski and Domcke^[15] on pyridine and pyrazine, and recent experimental studies by Zewail and co-workers^[5] on pyridine suggest the existence of a similar azaprefulvene structure in pyridine photochemistry involving the $S_2(\pi\pi^*)$ excited state. The existence of a Möbius pyridine structure in photoisomerization, however, has not been confirmed so far.

Using an approach similar to that employed by Sobolewski and Domcke,^[15] we located an azaprefulvene structure in dimethylpyridine by exchanging the alpha HOMO and the alpha LUMO in the UB3LY/6–311G** calculation. Despite the lack of any geometrical restriction (i. e. C_1 symmetry was employed), the optimized geometry of this azaprefulvene shows basically C_s symmetry. Frequency calculations show that this azaprefulvene structure is a transition state. Considering the biradical character of azaprefulvene, we reoptimized

the azaprefulvene structure with the CASSCF method. The CASSCF optimization within C_s symmetry located an azaprefulvene structure (Figure 3) with almost the same equilibrium geometry as the previous UB3LYP approach, but CASSCF frequency analysis shows that this azaprefulvene is a

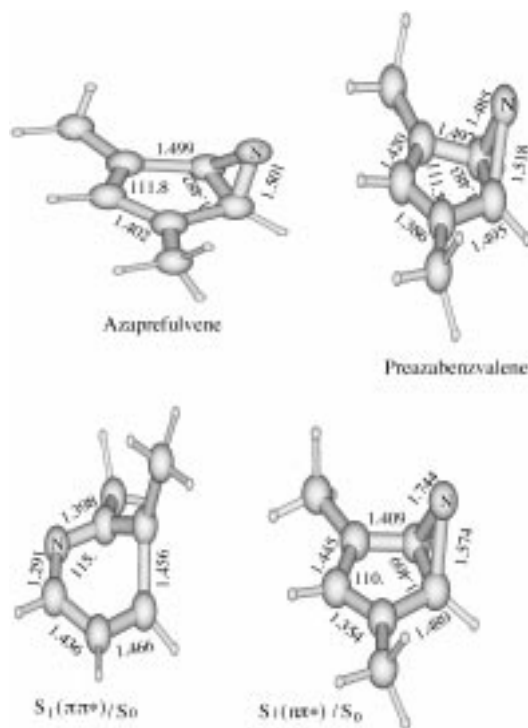


Figure 3. CASSCF-optimized geometries [\AA , $^\circ$] of azaprefulvene, preazabenzvalene, and the conical intersection minima.

stable minimum on the PES. This finding is consistent with previous studies on benzene and pyridine.^[15, 5] The ground state of this structure correlates according to the CASSCF wavefunction with the $S_1(n\pi^*)$ configuration in the parent **6**. The first and second excited states in this structure are close in energy, and correlate with the $S_2(\pi\pi^*)$ and the $S_0(\pi^2)$ configuration of the parent **6**, respectively. This observation suggests that the excited azaprefulvene corresponds to an $S_2(\pi\pi^*)/S_0(\pi^2)$ conical intersection or is located near an S_2/S_0 crossing surface.

In the vicinity of the azaprefulvene, a preazabenzvalene structure (Figure 3) was also found by the CASSCF calculation to be minimum on the PES. The preazabenzvalene and azaprefulvene intermediates are basically isoenergetic even though a significant difference in the out-of-plane angle exists. Analogous prefulvene and prebenzvalene structures connected by a relatively flat PES in the prefulvene biradical region has also been documented in an MC-SCF study of photochemical reactions of benzene.^[16a]

In a subsequent search for the conical intersection of **6** by CAS(6,6) calculations, an azabenzvalene-like structure (Figure 3) was found, and CASSCF calculations characterized it as an $S_1(n\pi^*)/S_0(\pi^2)$ conical minimum. This $S_1(n\pi^*)/S_0$ is about 44 kcal mol⁻¹ higher in energy than the azabenzvalene **10**. Thus, the azabenzvalene-like $S_1(n\pi^*)/S_0$ is likely to transform to the photoproduct azabenzvalene **10**.

To correlate formation of relevant intermediates with the low-lying excited states and to get some qualitative features of the adiabatic correlation of S_0 , S_1 , and S_2 in the photoisomerization process of **6**, we performed CAS(10,7) energy calculations along the path to the azabenzvalene-like structure $S_1(\pi\pi^*)/S_0(\pi^2)$. The adiabatic potential energy curve of S_0 rises along this path. The close-lying S_1 and S_2 show an interaction at the beginning of this pathway that is of a similar nature to that found by Sobolewski and Domcke^[5] for pyridine (rising $\pi\pi^*$ and descending $\pi\pi^*$ curve). This is then followed at a late stage on the path by the $S_1(\pi\pi^*)/S_0(\pi^2)$ conical crossing. These results suggest that the intermediate **10** is likely to be formed after excitation via the S_2/S_1 interaction followed by an S_1/S_0 decay. As mentioned before, the structure of excited azaprefulvene bears the character of an S_2/S_0 conical intersection. Thus, the azaprefulvene intermediate could be expected to be involved in the formation of the intermediate **10**. Recent experimental studies by Zewail et al.^[5] indicate that the azaprefulvene structure due to the $S_2(\pi\pi^*)$ is involved in the photoreaction of pyridine.

In the photoreaction of parent **2**, an $S_1(\pi\pi^*)/S_0$ conical intersection structure has been found along the path to Möbius dimethylpyridine **14**. This structure arises from the isomerization of the $\pi\pi^*$ excited state S_1 in **2**. Figure 3 shows the geometries of the azaprefulvene, preazabenzvalene, and conical intersection minima leading to the Möbius dimethylpyridine intermediate **14** and azabenzvalene intermediate **10**.

Formation of Dewar dimethylpyridine: Of three possible Dewar dimethylpyridines only **7** (Scheme 1) was detected by ¹H NMR spectroscopy. At the B3LYP/6–311G** level, **7** was found to be more stable than **8** and **9** by 0.5 and 7.4 kcal mol⁻¹, respectively. Figure 4 displays the relative energies for sta-

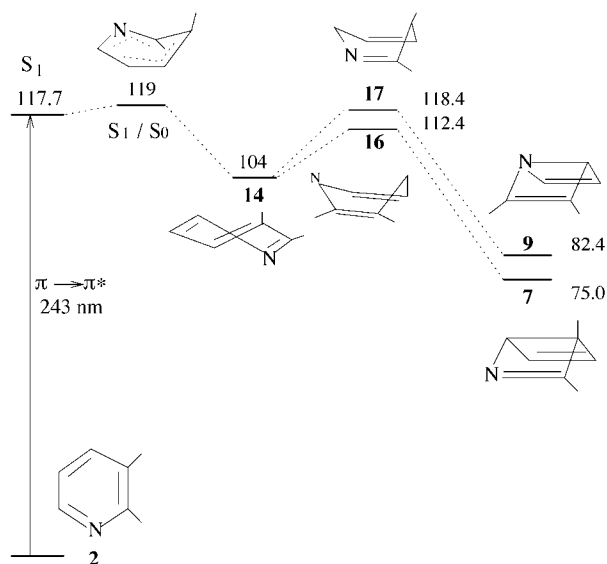


Figure 4. Relative energetics [kcal mol⁻¹] of the formation of Dewar dimethylpyridines.

tionary points on the PES from dimethylpyridine **2** to Dewar dimethylpyridines **7** and **9**. If dimethylpyridine **2** is excited to the $\pi\pi^*$ excited state S_1 , isomerization to Möbius dimethyl-

pyridine **14** can occur involving an S_1/S_0 conical intersection. In the present calculation, the $\pi-\pi^*$ vertical excitation occurs at 243 nm, slightly higher than the irradiation light of 254 nm. Considering a significant relaxation in geometry of the $\pi\pi^*$ excited state S_1 and an accuracy of no more than 0.2 eV, S_1 is certainly populated upon 254 nm irradiation. Isomerization to the Dewar form can involve the Möbius form **14**, or it can proceed directly from excited dimethylpyridine **2** to the Dewar forms **7** and **9** by 3–6 or 1–4 bonding as has been studied for the isomerization of benzene and [*n*]paracyclophanes ($n=5, 6, 7$) to their Dewar-analogues.^[31] Formation of **7** from **14** proceeds via a transition state **16** with a low barrier of 8.2 kcal mol⁻¹ at the B3LYP level, while **9** is formed through a transition state **17** with a barrier of 14.4 kcal mol⁻¹. Dewar dimethylpyridine **7** is more stable than **9** by 7.4 kcal mol⁻¹. These results show that the isomerization reaction to **7** is both kinetically and thermodynamically more favorable than the process to **9**. This is in agreement with the experiment in which only Dewar dimethylpyridine **7** was observed after irradiation of **2** at 254 nm in liquid solution.^[6]

Another Möbius dimethylpyridine isomer, **15**, was also located (Figure 1), 1.4 kcal mol⁻¹ higher than **14** at the B3LYP/6–311G** level. Isomer **15** could be converted into Dewar pyridines **8** via 2,5-bonding. A conceivable pathway, namely that Dewar pyridine is formed from the intermediate **10** is very unlikely. Structure **18** displays the transition state from **10** to Dewar pyridine, which occurs with a very high barrier of 89 kcal mol⁻¹. Hence, this process is much less favorable than other reactions involving structure **10** as we will see (vide infra).

Singlet migratory-insertion mechanism: The azabenzvalene intermediate **10**, originating from the S_1/S_0 decay subsequent to the S_2/S_1 mixing, might serve as a precursor of selective nitrogen migratory-insertion. Figure 5 shows the relative

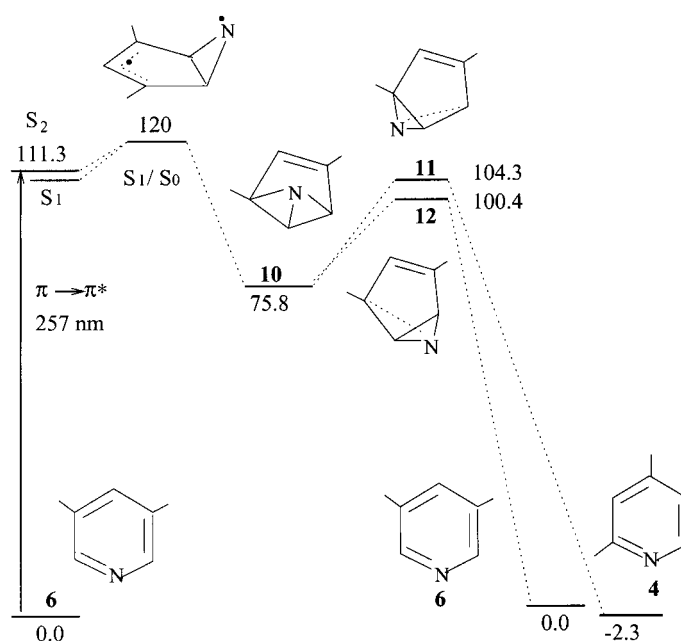
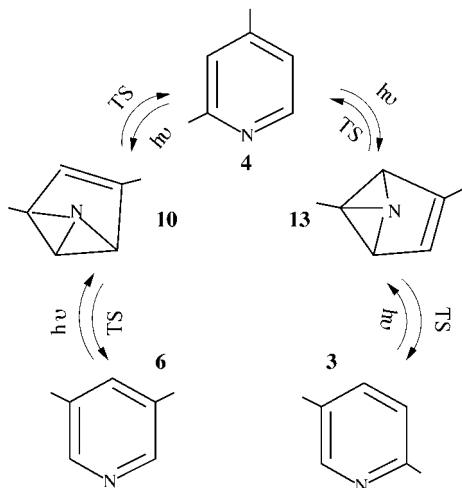


Figure 5. Relative energetics [kcal mol⁻¹] of the singlet phototransposition of **6** with **4** on the singlet potential energy surface.

energies of photoisomerization from **6** to **4** as well as reformation of **6** through **10**. In the suggested transposition mechanism, the reaction from **6** to **4** may proceed by generation of the intermediate **10** first, followed by nitrogen shifting insertion and rearomatization. The barrier is 28.6 kcal mol⁻¹ for the formation of **4** from **10**. A slightly lower barrier of 24.6 kcal mol⁻¹ is responsible for the isomerization from **10** back to **6**. Presumably, similar phototransposition processes from **4** to **6** and from **4** to **3** can take place via similar mechanisms. Scheme 4 displays the interconversion



Scheme 4. Interconversion mechanism of **6** with **4** and **3**.

mechanism of **6** with **4** and **3**. Notably, the mechanism shown in Scheme 4 is selective and no direct pathway connects **6** with **3**. This suggests that the existence of **4** is prerequisite for coexistence of **6** and **3** in photoisomerization products. Inspection of the photoproducts of **2** formed after irradiation at 254 nm shows that both **6** and **4** indeed do not exist, whilst the photoproducts were accompanied by the formation of **3**.^[6]

Triplet migratory-insertion mechanism: Two triplet ³(nπ*) and ³(ππ*) states of pyridine with different intrinsic lifetimes are observed experimentally.^[32] A strong vibronic coupling of the nearly degenerate ³(nπ*) and ³(ππ*) states may give rise to a pseudo Jahn–Teller type of interaction between these two states. This results in a double minimum in the lowest triplet surface, yielding a vibrationally relaxed triplet state with a boat-shaped geometry.^[33] Full CI and MP4 calculations with small basis sets show that the ³(nπ*) state is slightly more stable than the ³(ππ*) state. In the present work, it is found that higher nπ* and ππ* states of dimethylpyridine are also very close in energy (Table 2). In Table 3 we list energy minima and transition states that have been located by UB3LYP calculations for various forms involved in dimethylpyridine **6** isomerization. To judge the accuracy of the calculations and the radical character of these triplet stationary points on the PES, the spin population of these DFT calculations are also given.

The ³A₁(ππ*) state of **6** in planar geometry was found not to be a stable state at the UB3LYP level. Three imaginary frequencies correspond to in-plane deformation of the ring, the nitrogen out-of-plane distortion and wagging of aryl-H between the two methyl groups, respectively. The ³B₁(nπ*) state **28** in planar geometry was found to be a transition state at the UB3LYP/6–311G** level, which leads to an out-of-plane distortion geometry **19** following the imaginary mode. A similar triplet boat-shaped structure of pyridine was reported in a previous theoretical study.^[33]

Figure 6 shows the relative energetics on the triplet PES along the assumed photoisomerization path from **6** to **4**. The triplet state T₁(³B₁) in Figure 6 may be formed by either the direct S₀–T₁ excitation or by intersystem crossing (ISC) from S₁ → T₁ and from S₂ → T₁. The S₀–T₁ transition is formally spin forbidden, but can be enhanced by spin-orbit perturbation. Results of previous experimental studies show that the

Table 3. UB3LYP relative energies [kcal mol⁻¹], total spin and spin densities on nitrogen of triplet structures of dimethylpyridine **6**.

Species	19	20TS	21	22TS	23	24TS	25	26TS	27
ΔE	0.0	20.7	9.4	18.0	6.4	18.9	11.4	23.2	-1.6
S ²	2.02	2.01	2.03	2.05	2.08	2.05	2.03	2.02	2.02
ρ _s (N)	1.01	0.68	1.06	1.49	1.85	1.50	1.08	0.72	1.00

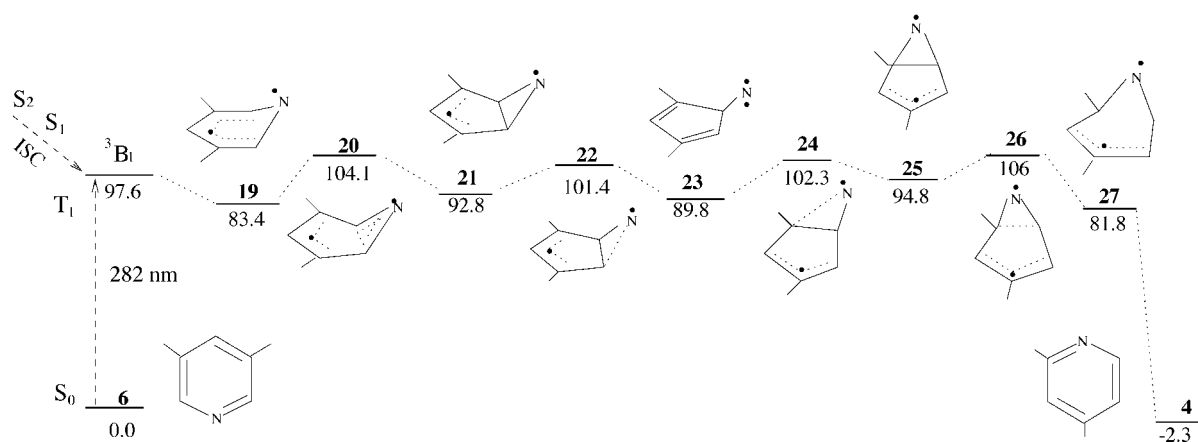


Figure 6. Relative energetics [kcal mol⁻¹] of the triplet phototransposition of **6** with **4** on the triplet potential energy surface calculated at the B3LYP/6–311G** level.

$T_1(^3B_1)$ state can be populated by ISC with a significant quantum yield.^[12]

In the present triplet transposition path, the triplet structure **19**, which is due to vibrational relaxation of the 3B_1 excited state, can be considered as a precursor in the triplet phototransposition from **6** to **4**. First, **19** proceeds to the azaprefulvene structure **21** via the transition state **20** with a barrier of 20.9 kcal mol⁻¹ (but only slightly above the energy of the 3B_1 state), followed by conversion from **21** to a more stable intermediate azafulvene **23** with a low barrier of 8.6 kcal mol⁻¹ (Figure 6). Then, another azaprefulvene **25** is formed through the transition state **24** with a barrier of 12.5 kcal mol⁻¹. Despite carefully searching for a direct transition state accounting for nitrogen shift from **21** to **25**, all attempts always find transition states **22** and **24**. This suggests that there should be no direct nitrogen migration from **21** to **25**. Finally, the azaprefulvene **25** is converted into the out-of-plane distortion geometry **27**, and subsequent rearomatization results in the formation of dimethylpyridine **4**. A similar triplet mechanism for the phototransposition of **4** to **3** could be schemed. This multistage transposition mechanism on the triplet PES is very likely since there are relatively low barriers for each step on the triplet PES, and furthermore the highest calculated barrier only requires an energy of 8 kcal mol⁻¹ above that of the 3B_1 state.

Conclusion

Plausible photochemical mechanisms of representative dimethylpyridines **2** and **6** have been suggested. In summary, a Möbius dimethylpyridine intermediate **14**, originating from photochemistry of the $\pi\pi^*$ excited state S_1 of **2**, may serve as the precursor to Dewar pyridine **7**. The isomerization to the product **7** is favored both kinetically and thermodynamically over the formation of other Dewar dimethylpyridines. The S_1/S_0 decay subsequent to the S_2/S_1 interaction in **6** yields an azabenzvalene intermediate **10** first, followed by nitrogen migration and rearomatization leading to **4**. Dimethylpyridine **4** may proceed to **3** by similar mechanisms with transposition of **6** with **4**. Electronic spectra due to valence-shell excitations in dimethylpyridines **2** and **6** have been estimated by CASPT2 and MRCI calculations. The vertical excitation energies of low-lying $^{1,3}(\pi\pi^*)$ and $^{1,3}(n\pi^*)$ excited states are compared with the irradiation light of 254 nm. The $^3(n\pi^*)$ photochemistry might be responsible for the interconversion of **6** with **4** on the triplet PES. A suggested multistage mechanism for selective nitrogen insertion involves electrocyclic ring closure, nitrogen migration around the sides of the cyclopentenyl ring, and rearomatization. Stable triplet intermediates, such as the out-of-plane distortion structures **19** and **27** originating from vibrational relaxation of the $^3(n\pi^*)$ excited state, triplet azaprefulvene biradicals **21** and **25**, and azafulvene **23** are all involved in the conversion from **6** to **4**. The photoisomerization channels proposed in the present study may be used to rationalize recent results from the photochemistry of dimethylpyridines and their analogues.

Acknowledgement

This work was supported by the National Science Foundation of China (Project Nos. 29773036 and 29892166). Z.C. gratefully acknowledges the Alexander von Humboldt Foundation for financial support during his stay in Universität Bonn. Some calculations were performed at the Institut für Physikalische Chemie und Theoretische Chemie, Universität Bonn.

- [1] S. Caplain, A. Lablache-Comber, *J. Chem. Soc. Chem. Commun.* **1969**, 1247.
- [2] K. E. Wilzbach, D. J. Rausch, *J. Am. Chem. Soc.* **1970**, *92*, 2178.
- [3] W. Roebke, *J. Phys. Chem.* **1970**, *74*, 4198.
- [4] D. Zhong, E. W.-G. Diao, T. Bernhardt, S. De Feyter, J. D. Roberts, A. H. Zewail, *Chem. Phys. Lett.* **1998**, *298*, 129.
- [5] M. Chachisvilis, A. H. Zewail, *J. Phys. Chem. A* **1999**, *103*, 7408, and references therein.
- [6] J. W. Pavlik, N. Kebede, M. Thompson, A. C. Day, J. A. Barltrop, *J. Am. Chem. Soc.* **1999**, *121*, 5666.
- [7] A. Bolovinos, P. Tsekeris, J. Philis, E. Pantos, G. Andritsopoulos, *J. Mol. Spectrosc.* **1984**, *103*, 240.
- [8] S. Japar, D. A. Ramsay, *J. Chem. Phys.* **1973**, *58*, 5832.
- [9] J. P. Doering, J. H. Moor, Jr., *J. Chem. Phys.* **1972**, *56*, 2176.
- [10] O. Kitao, H. Nakatsuji, *J. Chem. Phys.* **1988**, *88*, 4913.
- [11] a) J. Lorentzon, M. P. Fulscher, B. O. Roos, *Theor. Chim. Acta* **1995**, *92*, 67; b) I. C. Walker, M. H. Palmer, A. Hopkirt, *Chem. Phys.* **1989**, *141*, 365; c) J. B. Foresman, M. Head-Gordon, J. A. Pople, *J. Phys. Chem.* **1992**, *96*, 135.
- [12] a) I. Yamazaki, K. Sushida, H. Baba, *J. Chem. Phys.* **1979**, *71*, 381; b) I. Yamazaki, T. Murao, T. Yamanaka, K. Yoshihara, *Faraday Discuss.* **1983**, *75*, 395.
- [13] J. W. Pavlik, P. Tongcharoensirikul, N. P. Bird, A. C. Day, J. A. Barltrop, *J. Am. Chem. Soc.* **1994**, *116*, 2292.
- [14] P. J. MacLeod, A. L. Pincock, J. A. Pincock, K. A. Thompson, *J. Am. Chem. Soc.* **1998**, *120*, 6443.
- [15] A. L. Sobolewski, W. Domcke, *Chem. Phys. Lett.* **1991**, *180*, 381.
- [16] a) I. J. Palmer, I. N. Ragazos, F. Bernardi, M. Olivucci, M. A. Robb, *J. Am. Chem. Soc.* **1993**, *115*, 673; b) S. Kato, *J. Chem. Phys.* **1988**, *88*, 3045.
- [17] R. P. Johnson, K. J. Daoust, *J. Am. Chem. Soc.* **1996**, *118*, 7381.
- [18] A. D. Becke, *J. Chem. Phys.* **1993**, *98*, 5648.
- [19] C. Lee, W. Yang, R. G. Parr, *Phys. Rev.* **1988**, *B37*, 785.
- [20] B. O. Roos, M. P. Fulscher, P.-Å. Malmqvist, M. Merchán, L. Serrano-Andrés in *Quantum Mechanical Electronic Structure Calculations with Chemical Accuracy* (Eds.: S. R. Langhoff), Kluwer Academic Publishers, Dordrecht, The Netherlands, **1995**, p. 357.
- [21] a) R. I. Buenker, S. D. Peyerimhoff, *Theor. Chim. Acta* **1974**, *35*, 33; b) R. J. Buenker, S. D. Peyerimhoff, *Theor. Chim. Acta* **1975**, *39*, 217; c) R. J. Buenker, S. D. Peyerimhoff, W. Butscher, *Mol. Phys.* **1978**, *35*, 771.
- [22] a) R. J. Buenker, S. D. Peyerimhoff in *New Horizons of Quantum Chemistry* (Eds.: P. O. Löwdin, B. Pullman), Reidel, Dordrecht, **1983**; b) E. R. Davidson in *The Word of Quantum Chemistry* (Eds.: R. Daudel, B. Pullman), Reidel, Dordrecht, **1974**, p. 7.
- [23] M. J. Frisch, G. W. Trucks, H. B. Schlegel, P. M. W. Gill, B. G. Johnson, M. A. Robb, J. R. Cheeseman, T. Keith, G. A. Petersson, J. A. Montgomery, K. Raghavachari, M. A. Al-Laham, V. G. Zakrzewski, J. V. Ortiz, J. B. Foresman, C. Y. Peng, P. Y. Ayala, W. Chen, M. W. Wong, J. L. Andres, E. S. Replogle, R. Gomperts, R. L. Martin, D. J. Fox, J. S. Binkley, D. J. Defrees, J. Baker, J. P. Stewart, M. Head-Gordon, C. Gonzalez, J. A. Pople, Gaussian 94, Revision B.3, Gaussian Inc., Pittsburgh, PA, **1994**.
- [24] K. Andersson, M. R. A. Blomberg, M. P. Fulscher, G. Karlström, R. Lindh, P.-Å. Malmqvist, P. Neogrády, J. Olsen, B. O. Roos, A. J. Sadlej, M. Schütz, L. Seijo, L. Serrano-Andrés, P. E. Siegbahn, and P.-O. Widmark, MOLCAS Version 4, Lund University, Sweden, **1997**.
- [25] M. Hanrath, B. Engels, *Chem. Phys.* **1997**, *225*, 167.
- [26] A. D. McLean, G. S. Chandler, *J. Chem. Phys.* **1980**, *72*, 5639.
- [27] R. Krishnan, J. S. Binkley, R. Seeger, J. A. Pople, *J. Chem. Phys.* **1980**, *72*, 650.

- [28] P. Poirier, R. Kari, I. G. Csizmadia, *Handbook of Gaussian Basis Sets*, Elsevier, **1985**.
- [29] E. Farenhorst, *Tetrahedron Lett.* **1966**, 6465.
- [30] a) D. Bryce-Smith, A. Gilbert, *Tetrahedron* **1976**, 32, 1309; **1977**, 33, 2459; b) A. Gilbert, J. Baggott, *Essentials of Molecular Photochemistry*, Blackwell Scientific Publications, Boston, **1991**.
- [31] M. von Arnim, S. D. Peyerimhoff, *Theor. Chim. Acta* **1993**, 85, 43.
- [32] J. L. Selco, P. L. Holt, R. B. Weisman, *J. Chem. Phys.* **1983**, 79, 3269.
- [33] S. Naqaoka, U. Nagashima, *J. Phys. Chem.* **1990**, 94, 4467.

Received: June 5, 2000

Revised version: December 1, 2000 [F2526]